



The role of 5-R-1,10-phenanthroline (R = CH₃, NO₂) on the emission properties and second-order NLO response of cationic Ir(III) organometallic chromophores

Claudia Dragonetti^{a,c}, Stefania Righetto^{a,c}, Dominique Roberto^{a,c,d}, Renato Ugo^{a,c,d,*}, Adriana Valore^{a,c}, Francesco Demartin^b, Filippo De Angelis^e, Antonio Sgamellotti^e, Simona Fantacci^{e,*}

^a Dipartimento di Chimica Inorganica, Metallorganica e Analitica "Lamberto Malatesta", Università di Milano, Via Venezian 21, I-20133, Milano, Italy

^b Dipartimento di Chimica Strutturale e Stereochimica Inorganica dell'Università di Milano, Via Venezian 21, I-20133, Milano, Italy

^c UdR dell'INSTM di Milano, Via Venezian 21, I-20133, Milano, Italy

^d ISTM-CNR, via Venezian 21, Via Venezian 21, I-20133, Milano, Italy

^e ISTM-CNR and UdR dell'INSTM di Perugia, Dipartimento di Chimica, Via Elce di Sotto 8, I-06123, Perugia, Italy

ARTICLE INFO

Article history:

Received 28 January 2008

Received in revised form 9 March 2008

Accepted 11 March 2008

Available online 16 March 2008

This work is dedicated to Prof. Dante Gatteschi and to his outstanding contribution to the modern magnetic aspects of coordination chemistry.

Keywords:

Emission

Nonlinear optics

Cyclometallated iridium complexes

Phenanthroline complexes

DFT/TDDFT calculations

X-ray diffraction

ABSTRACT

[Ir(cyclometallated 4,5-diphenyl-2-methyl-thiazole)₂(5-R-1,10-phenanthroline)][PF₆] (R = CH₃, NO₂) complexes were prepared and fully characterized, the structure of the complex with 5-CH₃-1,10-phenanthroline being also determined by X-ray diffraction. The emission properties of both complexes have been investigated and their second-order nonlinear optical (NLO) response has been determined experimentally by the EFISH technique and found to be similar but slightly lower than that of related [Ir(ppy)₂(5-R-1,10-phenanthroline)][PF₆] (ppy = cyclometallated 2-phenylpyridine), characterized by one of the highest second-order NLO response ever reported for a metal complex. In the complexes, SOS/TDDFT calculations show that the large and negative sign of the measured hyperpolarizability is mainly due to the significant contribution of rather intense MLCT transitions involving the phenanthroline as acceptor ligand.

© 2008 Elsevier B.V. All rights reserved.

1. Introduction

Organometallic complexes with luminescent [1] and second-order nonlinear optical (NLO) [2] properties are of interest as molecular building blocks of composite materials for light emitting systems such as OLED or for electrooptical devices and optical communications. In particular, they can offer additional flexibility, when compared to organic NLO-phores, by introducing electronic charge-transfer transitions between the metal and the ligand, usually at relatively low energy and of relatively high intensity, tunable by virtue of the nature, oxidation state and coordination sphere of the metal centre [3].

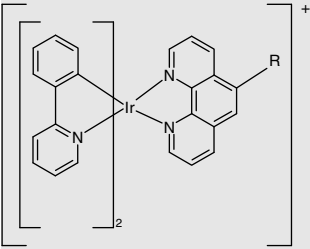
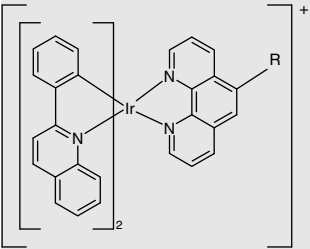
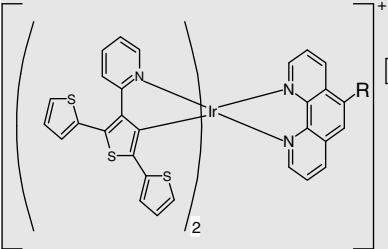
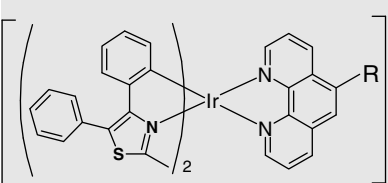
We previously reported that some cationic Ir(III) complexes of the type [Ir(ppy)₂(5-R-1,10-phenanthroline)][PF₆] (ppy = cyclo-

* Corresponding authors. Addresses: Dipartimento di Chimica Inorganica, Metallorganica e Analitica "Lamberto Malatesta", Via Venezian 21, I-20133, Milano, Italy (R. Ugo). ISTM-CNR, Via Elce di Sotto 8, I-06123, Perugia, Italy (S. Fantacci). Fax: +39 02 50314405.

E-mail addresses: dominique.roberto@unimi.it (R. Ugo), simona@thch.unipg.it (S. Fantacci).

metallated 2-phenylpyridine) are characterized by interesting luminescence properties [4] and large second-order NLO response [5], as determined by the electric field induced second harmonic generation method (EFISH) [6]. Good transparency towards the second harmonic emission renders these NLO-phores appealing as building blocks for composite second-order NLO materials [5]. The electronic origin of the second-order NLO response has been attributed by a theoretical SOS-TDDFT investigation mainly to metal to ligand charge transfer (MLCT) processes from the orbitals of the ppy-Ir based moiety acting as donor system to π^* orbitals of the coordinated phenanthroline acting as acceptor system. The second-order NLO response may be tuned by an adequate choice of the R substituent on the phenanthroline ligand, the best response being obtained with an electron-withdrawing substituent such as NO₂ (see complexes **1a–1b**, with R = Me and NO₂, respectively; Table 1) [5]. Substitution of cyclometallated 2-phenylpyridine with the more π -delocalized cyclometallated 2-phenylquinoline (pq) does not affect significantly both the luminescence properties and second-order NLO response (complexes **2a–2b**, with R = Me and NO₂, respectively; Table 1) whereas a slightly lower

Table 1
Absorption and emission spectra, ϕ and EFISH $\mu\beta_{1907}$ in CH_2Cl_2 for complexes **1–4**

Compound	Absorption max (nm) [ϵ ($\text{M}^{-1} \text{cm}^{-1}$)]	Emission max (nm)	Quantum yield σ	EFISH $\mu\beta_{1907}$ ^{a,b} ($10^{-30} \text{D cm}^5 \text{esu}^{-1}$)
	R = Me, 1a 255(sh), 268[60300], 333(sh), 377[8070], 410(sh) ^{c,d} R = NO₂, 1b 254(sh), 264[86900], 378[12400] ^{c,d}	559 ^c	38% ^c <0.1% ^c	–1565 ^e –2230 ^e
	R = Me, 2a 273[70400], 329[20700], 347(sh), 431[4750] ^{c,d} R = NO₂, 2b 268[81100], 324[27600], 430[6930] ^{c,d}	556 ^c	34% ^c <0.1% ^c	–2090 ^f –1720 ^f
	R = Me, 3a 260 [44500], 319(sh), 396[17378] ^{d,f} R = NO₂, 3b 257[62300], 315[28100], 397(sh) ^{d,f}	563 ^f	1.3% ^f <0.1% ^f	–1320 ^f –1640 ^f
	R = Me, 4a 261[48000], 272(sh), 358[9400] ^d R = NO₂, 4b 262[67200], 357[15200] ^d	586	12% <0.1%	–1414 –1780

^a EFISH measurements are carried out in CH_2Cl_2 at 10^{-3} M.

^b the error of EFISH measurements is $\pm 10\%$.

^c Ref. [4].

^d There is a band tail above 400 nm up to about 500–550 nm.

^e Ref. [5]

^f Ref. [7].

second-order NLO response and a much poorer luminescence was reported for the related Ir(III) complexes with the more π delocalized donor system of the cyclometallated 3'-(2-pyridil)-2,2':5',2''-terthiophene (ttpy) (complexes **3a–3b**, with R = Me and NO_2 , respectively; Table 1) [7]. In the present paper we extend our investigation to the emission properties and second-order NLO response of the series [Ir(cyclometallated 4,5-diphenyl-2-methylthiazole)₂(5-R-1,10-phenanthroline)][PF₆] (R = CH₃, NO_2 ; complexes **4a–4b**).

2. Experimental

2.1. General information

All reagents and solvents were purchased from Sigma–Aldrich, while IrCl_3 tri-hydrate was purchased from Engelhard. The Ir(III)

chloro-bridge dimer [Ir(cyclometallated 4,5-diphenyl-2-methylthiazole)₂Cl₂] was prepared following the procedure reported for [Ir(cyclometallated 2-phenylpyridine)₂Cl₂] [8] whereas the complexes [Ir(cyclometallated 4,5-diphenyl-2-methylthiazole)₂(5-R-1,10-phenanthroline)][PF₆] (R = Me, NO_2) were prepared with a procedure similar to that reported for this kind of cationic complexes [4,7]. The detailed synthetic procedure are reported below. All reactions were carried out under nitrogen atmosphere. ¹H NMR spectra were obtained on a Bruker Avance DRX 300 MHz instrument. Elemental analyses were carried out in the Dipartimento di Chimica Inorganica, Metallorganica e Analitica “Lamberto Malatesta” of the Milan University. EFISH measurements [6] were carried out in the same Department working in CH_2Cl_2 (10^{-3} M) at a non-resonant incident wavelength of 1.907 μm , using a Q-switched, mode-locked Nd³⁺:YAG laser manufactured by Atalaser equipped with a Raman shifter [5,7].

2.2. [Ir(cyclometallated 4,5-diphenyl-2-methyl-thiazole)₂Cl₂]

Iridium trichloride tri-hydrate (0.500 g) was combined with 4,5-diphenyl-2-methyl-thiazole (0.848 g; 3.35 mmol), dissolved in a mixture of 2-methoxyethanol (30 mL) and water (10 mL), and refluxed for 24 h. The solution was cooled to room temperature, and the yellow precipitate was filtered under nitrogen atmosphere. The precipitate was washed with 95% ethanol (60 mL) and acetone (60 mL) and then dissolved in dichloromethane (75 mL) and filtered. The desired product was obtained evaporating the solution to dryness (0.982 g, 80% yield). ¹H NMR (300 MHz, DMSO) 7.58 (s, 10H), 6.77 (d, *J* = 6.55, 1H), 6.59 (t, *J* = 8.57, 1H), 6.47 (t, *J* = 7.64, 1H), 6.17 (d, *J* = 7.69, 1H), 3.31 (s, 3H). *Anal. Calc.* for Ir₂C₆₄H₄₈N₄S₄Cl₂: C, 52.77; H, 3.32; N, 3.85. Found: C, 52.80; H, 3.33; N, 3.80%.

2.3. Synthesis of [Ir(cyclometallated 4,5-diphenyl-2-methyl-thiazole)₂(5-CH₃-1,10-phenanthroline)][PF₆] (**4a**)

A solution of [Ir(4,5-diphenyl-2-methyl-thiazole)₂Cl₂] (0.100 g, 0.0683 mmol) and 5-methyl-1,10-phenanthroline (0.0291 g, 0.1498 mmol) in CH₂Cl₂-MeOH (50 ml, 2:1 v/v) was heated to reflux. After 5–6 h, the orange solution was cooled to room temperature, and then a 10-fold excess of ammonium hexafluorophosphate was added. The suspension was stirred for 15 min, and then filtered to remove insoluble inorganic salts. The solution was evaporated to dryness under reduced pressure, affording an orange crude solid. The solid was redissolved in CH₂Cl₂ and filtered to remove the last traces of inorganic salts. Diethyl ether was layered onto the orange filtrate, and the mixture was cooled to ~0 °C. Orange-plates of the desired product were formed overnight and recovered by filtration (0.1057 g, 75% yield). ¹H NMR (300 MHz, CD₂Cl₂) δ 8.79 (dd, *J*₁ = 8.45, *J*₂ = 1.35, 1H), 8.60 (dd, *J*₁ = 8.25, *J*₂ = 1.35, 1H), 8.54 (dd, *J*₁ = 5.03, *J*₂ = 1.33, 1H), 8.46 (dd, *J*₁ = 8.37, *J*₂ = 5.05, 1H), 8.06 (s, 1H), 7.95 (dd, *J*₁ = 8.44, *J*₂ = 5.04, 1H), 7.88 (dd, *J*₁ = 8.25, *J*₂ = 5.06, 1H), 7.58 (s, 10 H), 7.22 (d, *J* = 7.86, 2H), 6.96 (m, 2H), 6.85 (m, 2H), 6.54 (dd, *J*₁ = 7.56, *J*₂ = 3.68, 2H), 2.98 (s, 3H), 1.54 (s, 6H). *Anal. Calc.* for Ir₁C₇₇H₃₄N₄S₂PF₆: C, 52.37; H, 3.32; N, 5.43. Found: C, 52.30; H, 3.29; N, 5.45%.

2.4. Synthesis of [Ir(cyclometallated 4,5-diphenyl-2-methyl-thiazole)₂(5-NO₂-1,10-phenanthroline)][PF₆] (**4b**)

A solution of [Ir(cyclometallated 4,5-diphenyl-2-methyl-thiazole)₂Cl₂] (0.0697 g, 0.0476 mmol) and 5-nitro-1,10-phenanthroline (0.0214 g, 0.095 mmol) in CH₂Cl₂-MeOH (50 ml, 2:1 v/v) was heated to reflux. After 5–6 h, the orange solution was cooled to room temperature, and then a 10-fold excess of ammonium hexafluorophosphate was added. The suspension was stirred for 15 min, and then filtered to remove insoluble inorganic salts. The solution was evaporated to dryness under reduced pressure, affording an orange crude solid which was redissolved in CH₂Cl₂ and filtered to remove the last traces of inorganic salts. Diethyl ether was layered onto the orange filtrate, and the mixture was cooled to ~0 °C. Orange-plates of the desired product were formed overnight and recovered by filtration (0.0778 g, 77% yield). ¹H NMR (400 MHz, CD₂Cl₂) δ 9.38 (dd, *J*₁ = 1.25, *J*₂ = 8.72, 1H), 9.18 (s, 1H), 8.93 (dd, *J*₁ = 1.00, *J*₂ = 8.15, 1H), 8.69 (ddd, *J*₁ = 1.17, *J*₂ = 5.03, *J*₃ = 16.35, 2H), 8.09 (dd, *J*₁ = 5.04, *J*₂ = 8.75, 2H), 7.59 (d, *J*₁ = 1.50, 10H), 7.23 (dd, *J*₁ = 1.10, *J*₂ = 7.90, 2H), 6.98 (m, 2H), 6.87 (m, 2H), 6.51 (m, 2H), 2.98 (s, 6H). *Anal. Calc.* for Ir₁C₄₄H₃₁N₅-S₂O₂PF₆: C, 49.71; H, 2.94; N, 6.59. Found: C, 49.67; H, 3.18; N, 6.21%.

2.5. Photophysical measurements

UV spectra were recorded at room temperature in a 1 cm quartz cuvette using a Jasco V-570 spectrometer. Emission spectra were recorded using a Jobin-Yvon Fluorolog-3 spectrometer equipped with double monochromators and Hamamatsu-928 photomultiplier tube (PMT) as the detector. All complexes were excited at 260 nm. Emission quantum yields have been determined, using the method of Demas and Crosby [9a] by comparison with the emission of Coumarine 540, employed as a standard [9b]. All solutions were de-aerated by nitrogen bubbling for 30 min before measurements.

2.6. X-ray determination of the structure of [Ir(cyclometallated 4,5-diphenyl-2-methyl-thiazole)₂(5-Me-1,10-phenanthroline)][PF₆] (**4a**)

Crystals of [Ir(cyclometallated 4,5-diphenyl-2-methyl-thiazole)₂(5-Me-1,10-phenanthroline)][PF₆], suitable for X-ray diffraction studies, were obtained by slow addition at room temperature of pentane to its solution in CH₂Cl₂.

2.6.1. Crystal data

C₄₅H₃₄F₆IrN₄PS₂ · 5CH₂Cl₂, *M* = 1074.51, monoclinic, *a* = 15.083(2), *b* = 14.223(2), *c* = 21.301(3) Å, β = 99.09(1)°, *U* = 4512.2(11) Å³, *T* = 292(2) K, space group *P*2₁/*n* (No. 14), *Z* = 4, μ = (Mo Kα) 3.208 mm⁻¹. 21036 reflections (5594 unique, *R*_{int} = 0.086) were collected at room temperature in the range 2.00 ≤ 2θ ≤ 52.06°, employing a 0.08 × 0.03 × 0.02 mm crystal fragment mounted on a Bruker Apex II area-detector diffractometer. Graphite monochromatized Mo Kα radiation (λ = 0.71073 Å) was used with the generator working at 45 kV and 40 mA.

Intensities were corrected for Lorentz-polarisation effects and empirical absorption correction (SADABS [10]; minimum transmission factor 0.798). The structure was solved by direct methods (SIR-97 [11]) and refined on *F*_o² with the SHELXL-97 [12] program (WINGX suite [13]). All non-hydrogen atoms were refined with anisotropic thermal parameters, while hydrogen atoms, located on the Δ*F* maps, were allowed to ride on their carbon atom. Final *R*₁ [*wR*₂] values of 0.0479 [0.1233] on 3434 reflections with *I* > 2σ(*I*) and 557 parameters and *S* = 1.001. The crystal examined contains clathrated CH₂Cl₂ molecules showing different orientations: only one majority model with occupancy close to 0.5 could be refined: the maximum residual electron density on the final Δ*F* map is 0.95 e Å⁻³ and is close to the position of the disordered solvent molecule. The minimum residual of -0.60 e Å⁻³ is instead close to the iridium atom. Selected interatomic distances are reported in Table 2.

2.7. Computational details

The geometries of complexes **4a** and **4b** were optimized without symmetry constraints by density functional theory (DFT) calculations using the BP86 exchange–correlation function [14,15], together with a TZP (DZP) basis set for Ir, S (N, C, O, H), including scalar-relativistic corrections as implemented in the ADF program [16]. On the optimized geometries, we performed single-point and Time Dependent DFT (TDDFT) calculations at the B3LYP/LANL2DZ level of theory [17,18] in dichloromethane solutions by means of the polarizable continuum model (PCM) solvation model [19], as implemented in the GAUSSIAN 03 (G03) program package [20]. Calculation of the lowest 100 singlet–singlet excitations at the ground state optimized geometries allowed us to simulate a large (up to below 230 nm) portion of the absorption spectrum. We computed also the lowest 10 singlet–triplet excitations at the ground state geometry; the oscillator strength of singlet–triplet transitions is set to zero, due to the neglect of the spin–orbit coupling. The sim-

Table 2
Selected interatomic distances (Å) and angles (°) for compound **4a**, together the corresponding optimized values

	X-ray	Theor.		X-ray	Theor.
Ir–N1	2.161(9)	2.173	N1–C5	1.348(14)	1.341
Ir–N2	2.149(10)	2.170	C5–C9	1.412(16)	1.412
Ir–N3	2.049(10)	2.071	N2–C9	1.341(14)	1.348
Ir–N4	2.050(9)	2.072			
Ir–C29	2.010(11)	2.017			
Ir–C45	2.012(11)	2.018			
N3–C15	1.322(14)	1.327	N4–C31	1.329(14)	1.327
N3–C17	1.398(14)	1.401	N4–C33	1.410(14)	1.401
C17–C24	1.468(16)	1.453	C33–C40	1.430(16)	1.452
C24–C29	1.425(16)	1.418	C40–C45	1.421(15)	1.418
C15–S1	1.682(13)	1.725	C31–S2	1.684(13)	1.724
S1–C16	1.728(13)	1.742	S2–C32	1.721(12)	1.742
C16–C17	1.365(16)	1.374	C32–C33	1.360(16)	1.374
P–F1	1.542(10)		P–F4	1.514(10)	
P–F2	1.545(10)		P–F5	1.552(10)	
P–F3	1.539(13)		P–F6	1.471(12)	
C29–Ir–C45	89.7(4)	91.9	C45–Ir–N4	79.7(4)	79.9
C29–Ir–N3	81.3(5)	80.0	N3–Ir–N4	172.6(4)	169.6
C45–Ir–N3	93.8(4)	92.6	C29–Ir–N2	96.0(4)	95.7
C29–Ir–N4	94.8(4)	92.9	C45–Ir–N2	174.0(4)	172.2
N3–Ir–N2	85.4(4)	86.7	N4–Ir–N2	101.4(4)	101.4
C29–Ir–N1	172.1(4)	171.8	N3–Ir–N1	100.2(4)	101.3
C45–Ir–N1	97.9(4)	96.1	N4–Ir–N1	84.4(4)	87.1
N2–Ir–N1	76.5(4)	76.3	Ir–N1–C5	114.4(8)	114.3
N1–C5–C9	116.2(12)	117.8	C5–C9–N2	119.5(12)	117.0
C9–N2–Ir	113.3(8)	114.5	Ir–N3–C17	114.9(8)	114.7
N3–C17–C24	114.0(11)	114.8	C17–C24–C29	115.2(11)	114.5
C24–C29–Ir	114.5(9)	115.9	C15–N3–C17	110.8(11)	113.3
N3–C17–C16	114.7(12)	113.5	C17–C16–S1	108.8(10)	109.7
C16–S1–C15	91.3(7)	91.1	S1–C15–N3	114.4(10)	112.4
Ir–N4–C33	114.3(8)	114.8	N4–C33–C40	115.0(11)	114.7
C33–C40–C45	114.0(11)	114.5	C40–C45–Ir	115.8(9)	116.0
C31–N4–C33	112.1(10)	113.3	N4–C33–C32	113.0(11)	113.5
C33–C32–S2	110.1(9)	109.7	C32–S2–C31	91.6(6)	91.1
S2–C31–N4	113.1(9)	112.4			

ulation of the absorption spectrum of complex **4a** has been performed by a Gaussian convolution with FWHM = 0.4 eV; the related experimental spectrum have been rescaled so that the intensity of the experimental and theoretical main bands in the absorption spectrum matches. The quadratic hyperpolarizability (β) can be evaluated using a Sum Over States (SOS)-TDDFT approach [21]. This approach requires in principle the calculation of dipole matrix elements between all possible couples of excited states (three level terms), in addition to the ground to excited states transition dipole moments (two level terms) [22]. It turns out, however, that two- and three-level terms show approximately the same scaling with the number of excited states as two-level terms, so that the latter can be used for a semi-quantitative assessment of the major contributions to the quadratic hyperpolarizability. In the present study, we calculated the lowest excited states and ground state dipole moments for **4a** and **4b**. Ground and excited states dipole moments were computed from the SCF and Rho-Cl density, respectively.

3. Results and discussion

Complexes **4a** and **4b** were prepared according to the synthetic method previously reported [4] in two steps: (i) preparation of the chloro-bridge dimer $[\text{Ir}(\text{cyclometallated } 4,5\text{-diphenyl-2-methyl-thiazole})_2\text{Cl}]_2$ following the procedure reported for $[\text{Ir}(\text{ppy})_2\text{Cl}]_2$ [8]; (ii) bridge splitting reaction with a 5-R-1,10-phenanthroline (R = CH₃, NO₂; see Section 2). The structure of complex **4a** was determined by X-ray diffraction of suitable crystals which contain $[\text{Ir}(\text{cyclometallated } 4,5\text{-diphenyl-2-methyl-thiazole})_2(5\text{-Me-1,10-phenanthroline})]^+$ cations, PF₆⁻ anions and disordered CH₂Cl₂ molecules, separated by normal van der Waals interactions, in the

molar ratio 1:1:0.5, respectively. A perspective view of the cation is reported in Fig. 1. The iridium atom displays a distorted octahedral coordination geometry being surrounded by two cyclometallated 4,5-diphenyl-2-methyl-thiazolato ligands coordinated through the nitrogen atom of the thiazole moiety and one ortho carbon atom of the phenyl substituent at position 5 and by the chelated 5-Me-1,10-phenanthroline ligand. Within the thiazolato ligands one of the two phenyl substituents (that at position 5) lies essentially in the plane of the thiazole ring, whereas the plane of the phenyl at position 4 is almost normal to the average plane of the thiazole ring [S1–C16–C18–C19 torsion angle is $-100.7(16)^\circ$ and S2–C32–C34–C35 is $89.3(16)^\circ$]. The thiazole ring in both ligands does not deviate significantly from planarity. The two Ir–N1 and Ir–N2 distances of the phenanthroline ligand are significantly larger than the Ir–N distances of the two thiazolato moieties being *trans* to the C29 and C45 atoms σ -linked to Ir. The average P–F distance in the PF₆⁻ anion is 1.527 Å; P–F distances up to 1.73 Å have been reported only when this anion strongly interacts with its surrounding through hydrogen bonds (for instance in HPF₆·6H₂O [23]). Here, the value of 1.527 Å is in line with the shortest distances found in well isolated PF₆⁻ anions.

The main optimized geometrical parameters of complex **4a** obtained by theoretical DFT calculations are reported in Table 2, together with the related data obtained by the X-ray investigations, showing an excellent agreement between the experimental and computed data. The computed optimized molecular structure of complex **4b** is quite similar to that computed for complex **4a**, both in terms of bond lengths and angles.

Both complexes **4a** and **4b** show two intense absorption bands around 260–270 and 360 nm, respectively. This is a typical trend of this kind of cationic Ir(III) complexes such as **1a–1b** and **3a–3b** [4,5,7]. These latter show a small red-shift of the absorption at lower energy (from around 360 to around 395–400 nm), while, for **2a–2b** the band at lower energy shows a more pronounced red shift at around 430 nm (see Table 1). Complex **4a** shows, as all the other Ir(III) complexes **1a**, **2a**, **3a** containing 5-CH₃-1,10-phenanthroline [4,7], a emission around 586 nm with a quantum yield of 12%, lower than that of **1a** and **2a** (see Table 1) but high enough for the preparation of a single-layer electroluminescent device [24]. Complex **4b**, as all the other Ir(III) complexes **1b**, **2b**, **3b** containing 5-NO₂-1,10-phenanthroline [4,7], is not emissive (Table 1).

The second-order NLO response of **4a** and **4b** was measured in CH₂Cl₂ by the EFISH technique [6] working with a non-resonant 1907 nm incident wavelength. Comparison of the $\mu\beta$ values of **4a–4b** with those of related cationic NLO-phores **1a**, **2a**, **3a–1b**, **2b**, **3b** (Table 1) evidences that the cyclometallated 4,5-diphenyl-2-methyl-thiazole leads to a second-order NLO response slightly higher than that reported for the related complexes with the cyclometallated 3'-(2-pyridil)-2,2':5',2''-terthiophene (complexes **3a–3b**) but still slightly lower than those reported in the case of cyclometallated 2-phenylpyridine (complexes **1a–1b**).

To provide insights into the effects of the different nature of the cyclometallated ligands on the electronic transitions controlling the second-order NLO properties of this kind of complexes and in particular of **4a–4b**, we performed DFT/TDDFT calculations. The orbital energy levels of complexes **1a–1b**, **2a–2b**, **3a–3b**, **4a–4b**, obtained at a consistent level of theory, are reported in Fig. 2, together with the density plots of selected molecular orbitals of **4a** and **4b**. The highest occupied molecular orbital (HOMO) of both **4a** and **4b** is, as previously found for **1a**, **2a**, **3a** and **1b**, **2b**, **3b** [4,5,7] and related complexes [25–27], a $t_{2g}(\text{Ir})$ orbital mixed with a π orbital of the cyclometallated ligand (4,5-diphenyl-2-methyl-thiazole in the present case). In particular, assuming that the phenanthroline ligand is lying in the *xy* plane, with the *x* axis pointing from the metal to the ligand, the HOMO is originated from the d_{xy}

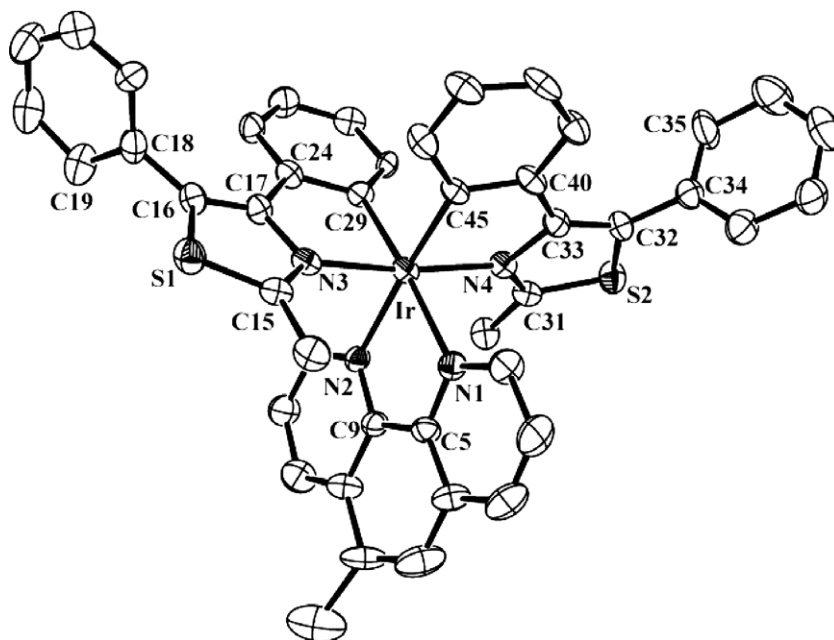


Fig. 1. ORTEP view of the $[\text{Ir}(\text{cyclometallated } 4,5\text{-diphenyl-2-methyl-thiazole})_2(5\text{-Me-1,10-phenanthroline})]^+$ cation with displacement ellipsoids at 25% probability.

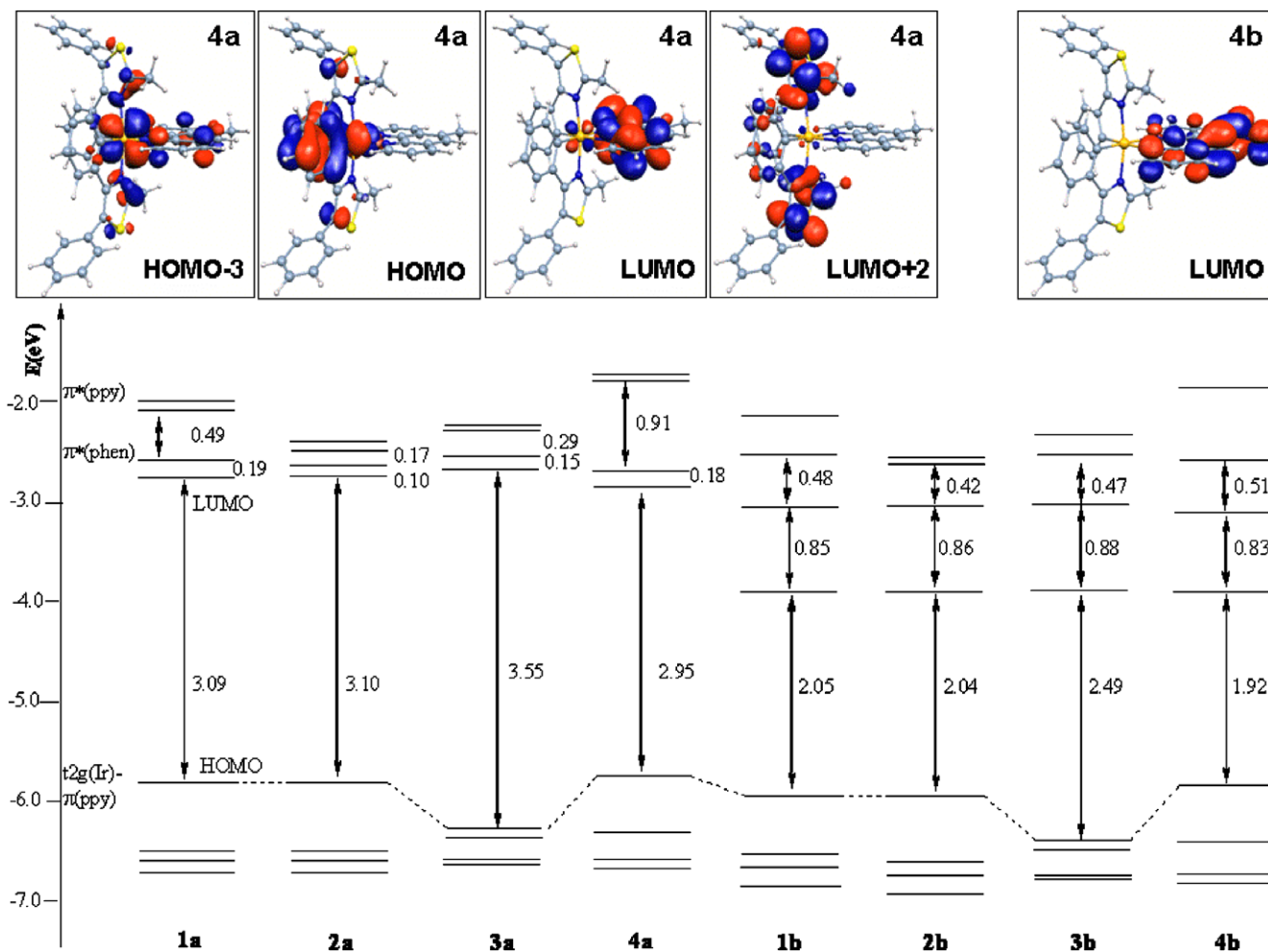


Fig. 2. Schematic representation of the frontier molecular orbitals of complexes 1–4. For complexes 4a isodensity plots of the HOMO – 3, HOMO, LUMO, and LUMO + 2 are reported. For complex 4b isodensity plot of LUMO is shown.

metal orbital, with the almost degenerate d_{xz} – d_{yz} orbitals lying ca. 1.0 eV below, being the HOMO – 3/HOMO – 4 (see Fig. 2). The HOMO – 1/HOMO – 2 are, on the other hand, π orbitals of the cyclometallated ligand (not shown in Fig. 2). The lowest unoccupied molecular orbital (LUMO) and LUMO+1 of **4a**, separated by 0.18 eV, are, as previously observed [4,5,7], phenanthroline π^* orbitals, with the LUMO showing some metal character reflecting π backdonation (see Fig. 2). The almost degenerate LUMO + 2/LUMO + 3 couple are π^* orbitals of the cyclometallated ligands, mainly localized on the thiazole ring (see Fig. 2). For **4b** the presence of the NO₂ phenanthroline substituent leads, as previously observed [4,5,7] to a substantial stabilization of the LUMO which translates into a significant reduction of the HOMO–LUMO gap for **4b** compared to **4a** (1.92 versus 2.95 eV).

A comparison between the experimental and TDDFT calculated absorption spectrum in CH₂Cl₂ for **4a** is reported in Fig. 3. The calculated spectrum (absorption bands at 372 and 253 nm) is in excellent agreement with the experimental one (absorption bands at 358 and 272 nm). As in the experimental spectrum, the band calculated at 253 nm is almost five times more intense than that at 372 nm. The 230 nm band found in the experimental spectrum is not reproduced by TDDFT due to the limited number of calculated excited states, which allowed us to reach only transitions below 230 nm. Inspection of the TDDFT eigenvectors allows the assignment of the character of the absorption bands. The two lowest calculated transitions of singlet and triplet character are at 548–556 and 489–493 nm, respectively, and correspond to HOMO → LUMO and HOMO → LUMO + 1 transitions. The singlet transitions show negligible oscillator strengths (those for the triplet transitions are set to zero due to the neglect of spin–orbit coupling) so that they are possibly related to the band tail extending into the visible region observed experimentally. The 372 nm band is originated essentially by an intense HOMO – 3 → LUMO transition ($f = 0.124$) of metal to ligand charge transfer (MLCT) character since it involves a transition from the Ir d_{xz} orbital to the lowest phenanthroline π^* orbital. The 272 nm experimental band appears to be composed by an envelop of intense $\pi - \pi^*$ transitions, in the range 294–246 nm, located on the cyclometallated ring and on the phenanthroline ligand.

The experimental absorption spectrum of **4b** is quite similar to that of **4a**, apart from the tail decaying into the visible region which is more intense for the former. A HOMO – 3 → LUMO transition at 511 nm ($f = 0.025$), missing in the spectrum of **4a**, was calculated in addition to the same pattern of MLCT and $\pi - \pi^*$ transitions calculated for **4a**, even though in the case of **4b** the experimental band at 357 nm was related to two overlapping bands calculated at ca. 380 and 320 nm, respectively.

To compute the contribution of singlet excited states to the quadratic hyperpolarizability (β), we used the SOS method in the case of related cationic Ir(III) complexes [5], which showed how the ILCT and MLCT transitions contribute with a different sign to β . In analogy with these previous SOS-TDDFT calculations carried out on **1b** [5], the second-order NLO response of **4a** and **4b** must be still controlled by the rather intense and low energy MLCT transitions involving HOMO–LUMO charge transfer processes from the cyclometallated moiety to the phenanthroline ligand. Therefore in the present study we limited our investigation to the lowest excited states which give rise to the MLCT absorption band of **4a** and **4b** spectra. Such approximate approach allows us to estimate the contribution of the lowest MLCT excitations to β and thus to visualize the charge transfer flow accompanying these electronic transitions. This seems a good approximation for **4a** and **4b**, where no competing ILCT/MLCT processes are computed, which on the contrary were present in the case of [Ir(cyclometallated 2-phenylpyridine)₂(5-NMe₂-1,10-phenanthroline)] [PF₆]₂ due to the presence of the NMe₂ substituent [5].

The increased value of the second-order NLO response of **4b** compared to **4a** must be thus related to the decreased HOMO–LUMO gap of **4b**, which provides an increased NLO response according to the SOS approach. To visualize the charge transfer process giving rise to the second-order NLO response, in Fig. 4 we report isodensity plots of the electron density difference between selected singlet excited states involved in the MLCT processes and the ground state of complexes **4a** and **4b**. A blue (red) color indicates a decrease (increase) of the electron density upon excitation, thus allowing visual inspection of the charge density flow accompanying electron excitations. Also in Fig. 4 are reported dipole moment differences between the excited and ground state,

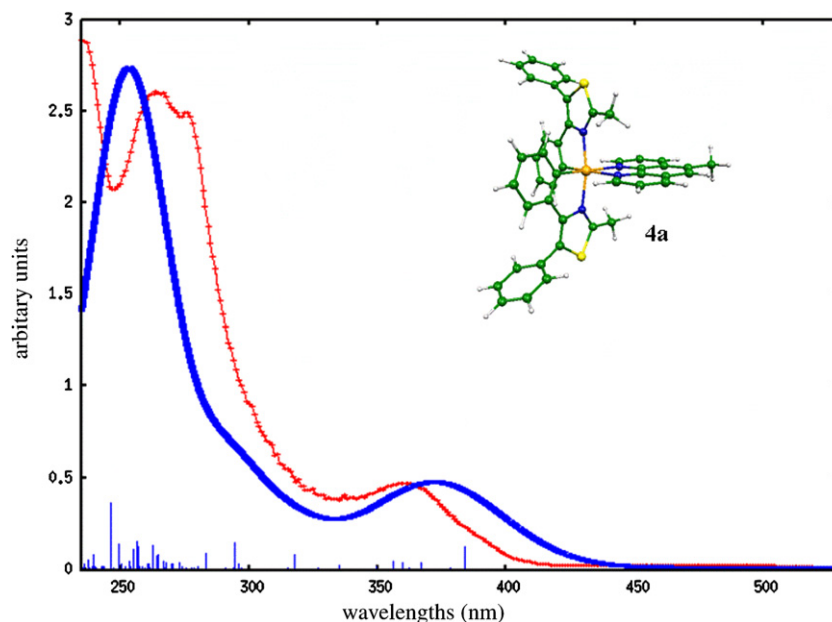


Fig. 3. Comparison between the experimental (red line) and computed (blue line) absorption spectra of **4a** complex. The experimental spectrum has been rescaled so that the intensity of the 272 nm band of the experimental spectrum matches the theoretical main feature.

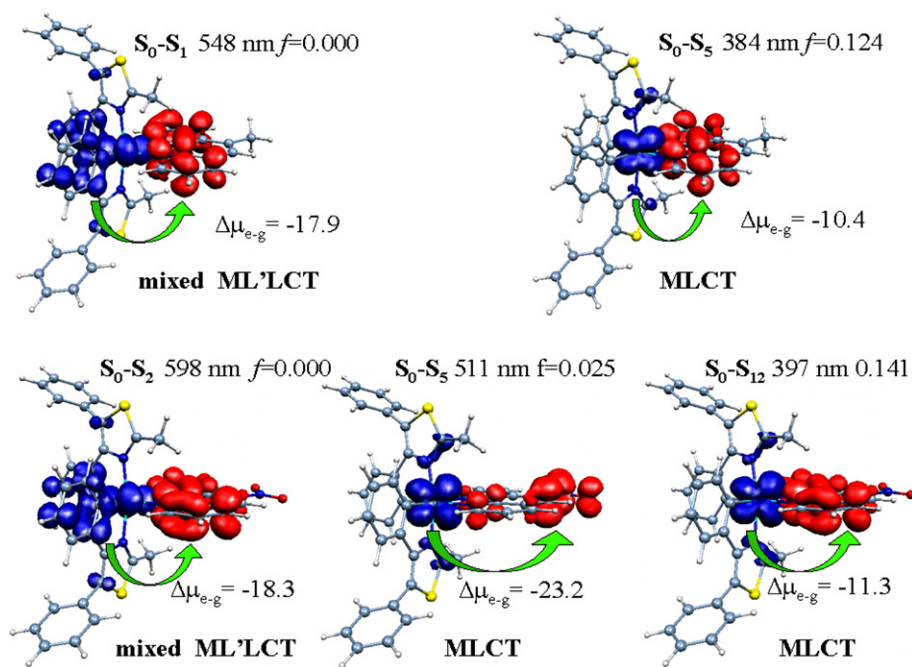


Fig. 4. Isodensity plots of the electron density difference between selected singlet excited states and the ground state of complexes **4a** (top) and **4b** (bottom). A blue (red) color indicates a decrease (increase) of the electron density upon excitation. The dominating x component of the dipole moment differences between the excited and ground state, excitation wavelengths, oscillator strengths and the character of the considered excitations are also reported.

whose negative sign, characteristic of MLCT excitations, gives rise to the negative sign of the second-order NLO response, according to a negative quadratic hyperpolarizability.

In summary, this work confirms that the second-order NLO response of these cationic cyclometallated Ir(III) complexes with 5-R-1,10-phenanthrolines is not strongly affected by the nature of the cyclometallated moiety whereas it is controlled and tuned by the nature of the R substituent on the phenanthroline ring. We also confirmed that the quantum yield of the emission is also controlled mainly by the nature of the R substituent on the phenanthroline ring.

4. Supplementary material

CCDC 675304 contains the supplementary crystallographic data for this paper. These data can be obtained free of charge from The Cambridge Crystallographic Data Centre via www.ccdc.cam.ac.uk/data_request/cif.

Acknowledgements

We thank for financial support the Ministero dell'Istruzione, dell'Università e della Ricerca (Programma di ricerca FIRB, year 2003, Research Title: Molecular compounds and hybrid nanostructured materials with resonant and non-resonant optical properties for photonic devices) and CNR (PROMO 2006).

References

- [1] R.C. Evans, P. Douglas, C. Winscom, *Coord. Chem. Rev.* 250 (2006) 2093.
- [2] (a) J. Zyss, *Molecular Nonlinear Optics: Materials, Physics and Devices*, Academic Press, Boston, 1994; (b) D.M. Roundhill, J.P. Fackler Jr. (Eds.), *Optoelectronic Properties of Inorganic Compounds*, Plenum Press, New York, 1999.
- [3] for example see (a) D.R. Kanis, P.G. Lacroix, M.A. Ratner, T.J. Marks, *J. Am. Chem. Soc.* 116 (1994) 10089; (b) J. Heck, S. Dabek, T. Meyer-Friedrichsen, H. Wong, *Coord. Chem. Rev.* 190–192 (1999) 1217; (c) H. Le Bozec, T. Renouard, *Eur. J. Inorg. Chem.* (2000) 229; (d) P.G. Lacroix, *Eur. J. Inorg. Chem.* (2001) 339; (e) S. Di Bella, *Chem. Soc. Rev.* 30 (2001) 355; (f) B.J. Coe, in: J.A. McCleverty, T.J. Meyer (Eds.), *Comprehensive Coordination Chemistry II*, vol. 9, Elsevier Pergamon Press, Oxford, UK, 2004, p. 621; (g) B.J. Coe, N.R.M. Curati, *Comments Inorg. Chem.* 25 (2004) 147; (h) E. Cariati, M. Pizzotti, D. Roberto, F. Tessore, R. Ugo, *Coord. Chem. Rev.* 250 (2006) 1210; (i) B.J. Coe, *Acc. Chem. Res.* 39 (2006) 383.
- [4] C. Dragonetti, L. Falciola, P. Mussini, S. Righetto, D. Roberto, R. Ugo, A. Valore, F. De Angelis, S. Fantacci, A. Sgamellotti, M. Ramon, M. Muccini, *Inorg. Chem.* 46 (2007) 8533.
- [5] C. Dragonetti, S. Righetto, D. Roberto, R. Ugo, A. Valore, S. Fantacci, A. Sgamellotti, F. De Angelis, *Chem. Commun.* (2007) 4116.
- [6] I. Ledoux, J. Zyss, *J. Chem. Phys.* 73 (1982) 203.
- [7] C. Dragonetti, S. Righetto, D. Roberto, A. Valore, T. Benincori, F. Sannicolò, F. De Angelis, S. Fantacci, *J. Mater. Sci.: Mater. Electron.* (2008), doi:10.1007/s10854-008-9670-9.
- [8] S. Sprouse, K.A. King, P.J. Spellane, R.J. Watts, *J. Am. Chem. Soc.* 106 (1984) 6647.
- [9] (a) J.N. Demas, G.A. Crosby, *J. Phys. Chem.* 75 (1971) 991; (b) R.F. Kubin, A.N. Fletcher, *Chem. Phys. Lett.* 99 (1983) 49.
- [10] SADABS Area-Detector Absorption Correction Program, Bruker AXS Inc., Madison, WI, USA, 2000.
- [11] A. Altomare, M.C. Burla, M. Camalli, G.L. Cascarano, C. Giacovazzo, A. Guagliardi, A.G.G. Moliterni, G. Polidori, R. Spagna, *J. Appl. Crystallogr.* 32 (1999) 115.
- [12] G.M. Sheldrick, *SHELX97 – Programs for Crystal Structure Analysis* (Release 97-2), University of Göttingen, Germany, 1998.
- [13] L.J. Farrugia, *J. Appl. Crystallogr.* 32 (1999) 837.
- [14] A.D. Becke, *Phys. Rev. A* 38 (1988) 3098.
- [15] J.P. Perdew, *Phys. Rev. B* 33 (1986) 8822.
- [16] G. te Velde, F.M. Bickelhaupt, E.J. Baerends, C. Fonseca-Guerra, S.J.A. van Gisbergen, J.G. Snijders, T. Ziegler, *J. Comput. Chem.* 22 (2001) 931.
- [17] A.D. Becke, *J. Chem. Phys.* 98 (1993) 5648.
- [18] P.J. Hay, W.R. Wadt, *J. Chem. Phys.* 82 (1985) 270.
- [19] S. Miertus, S. Scrocco, T. Tomasi, *Chem. Phys.* 55 (1981) 117.
- [20] M.J. Frisch, *GAUSSIAN 03*, Revision B.05, Gaussian Inc., Wallingford, CT, 2004.
- [21] A. Willetts, J.E. Rice, D.M. Burland, D.P. Shelton, *J. Chem. Phys.* 97 (1992) 7590.
- [22] D.R. Kanis, M.A. Ratner, T.J. Marks, *Chem. Rev.* 94 (1994) 195.
- [23] H. Bode, G. Teufer, *Acta Crystallogr.* 8 (1955) 611.
- [24] M. Muccini, A. Sharma, V. Shukla, E. Margapoti, C. Dragonetti, D. Roberto, R. Ugo, A. Valore, Unpublished results.
- [25] M.K. Nazeeruddin, R.T. Wegh, Z. Zhou, C. Klein, Q. Wang, F. De Angelis, S. Fantacci, *Inorg. Chem.* 45 (2006) 9245.
- [26] F. De Angelis, S. Fantacci, N. Evans, C. Klein, S.M. Zakeeruddin, J.-E. Moser, K. Kalyanasundaram, H. Bolink, M. Grätzel, M.K. Nazeeruddin, *Inorg. Chem.* 46 (2007) 5989.
- [27] D. Di Censo, S. Fantacci, F. De Angelis, C. Klein, N. Evans, K. Kalyanasundaram, H.J. Bolink, M. Grätzel, M.K. Nazeeruddin, *Inorg. Chem.* 47 (2008) 980.